



Supplement of

Measurement report: The effect of aerosol chemical composition on light scattering due to the hygroscopic swelling effect

Rongmin Ren et al.

Correspondence to: Zhanqing Li (zli@atmos.umd.edu)

The copyright of individual parts of the supplement might differ from the article licence.

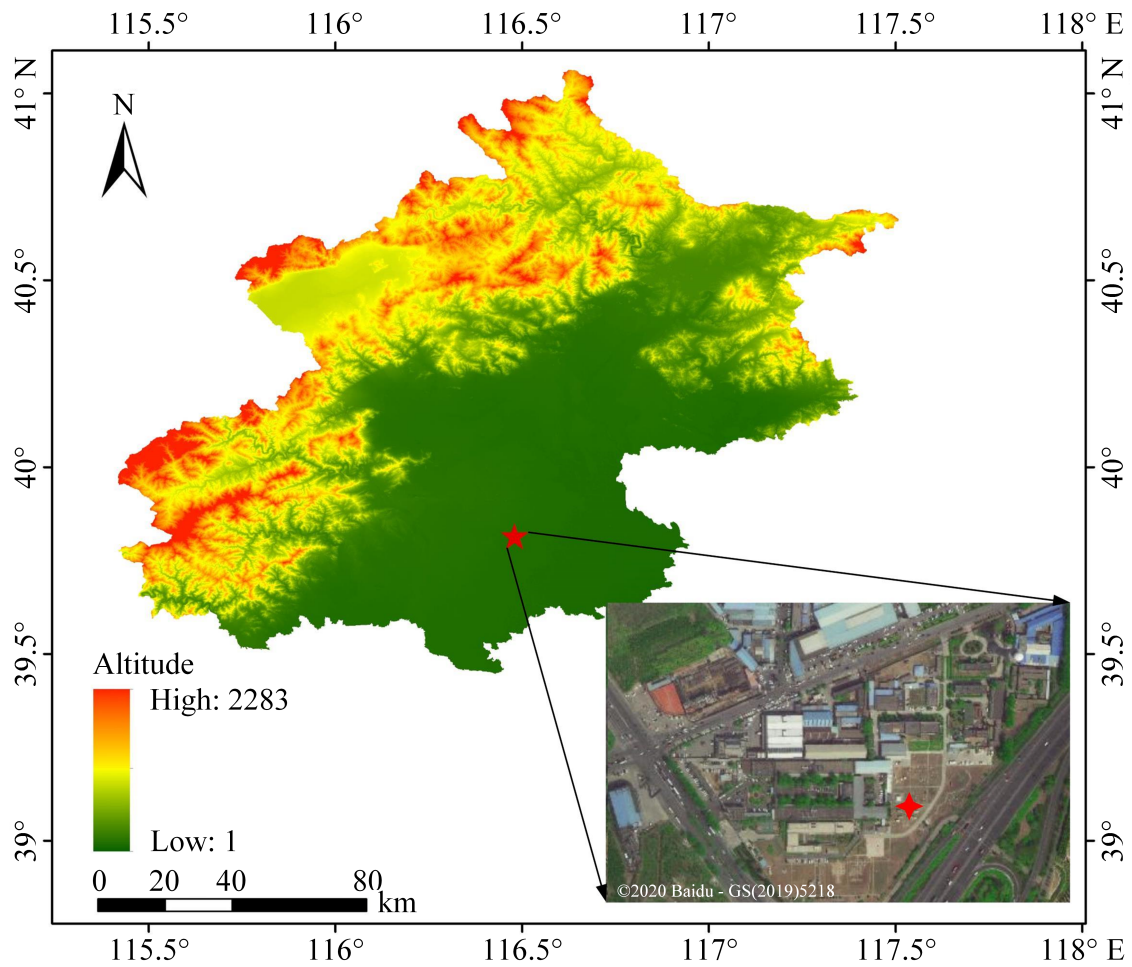
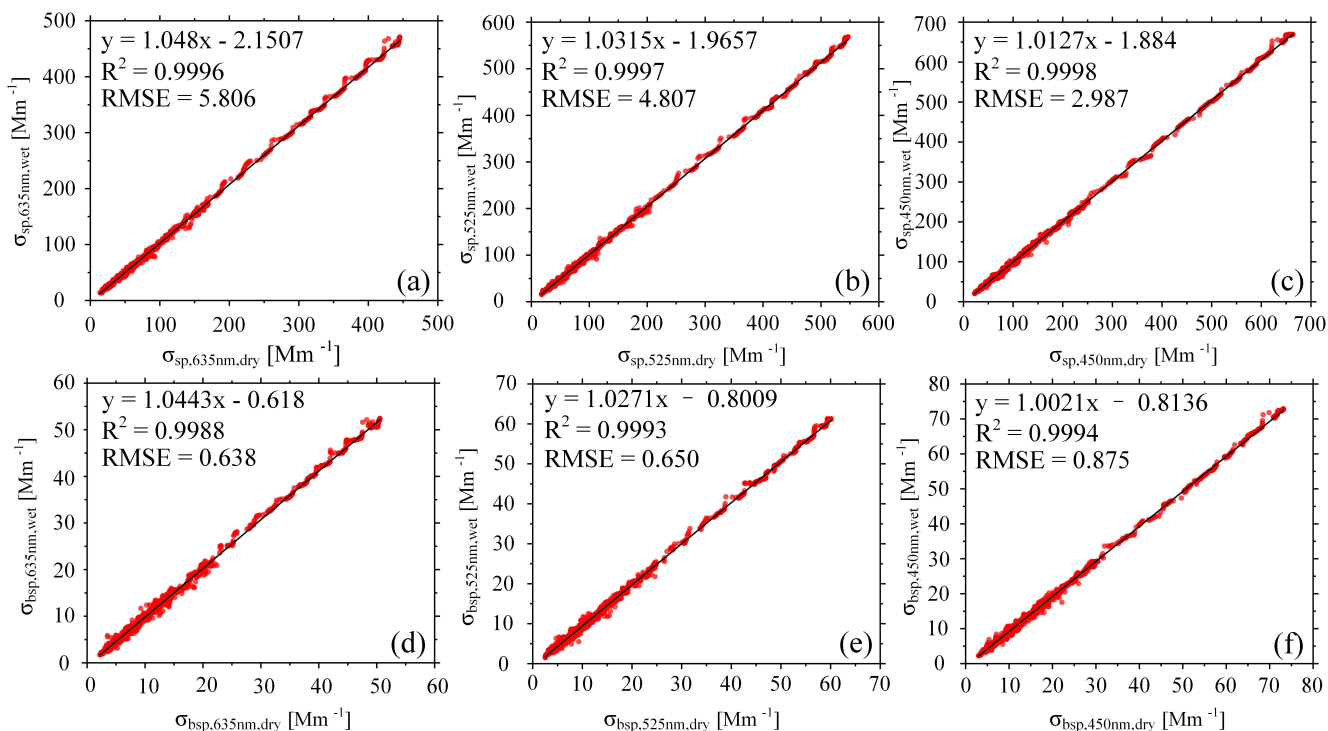
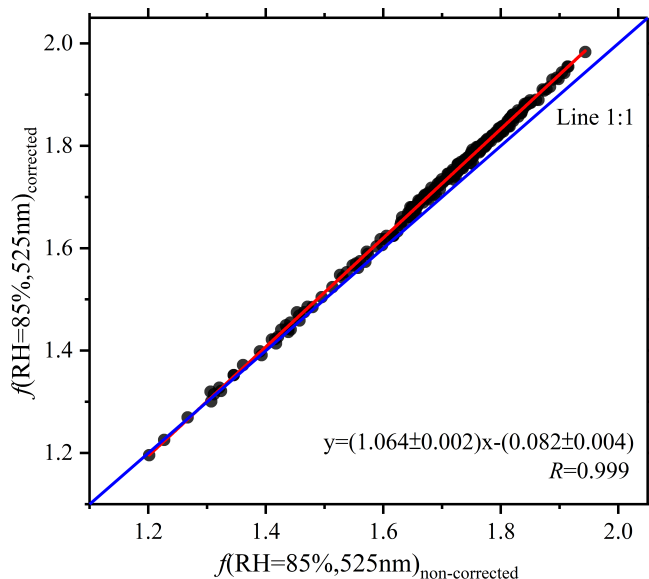


Figure S1: Map of the terrain heights of Beijing, China (unit: m above sea level). The red star shows the position of the observatory, and the image in the lower right corner is a true-color image of the observatory surroundings.

The scattering and backscattering coefficients at three wavelengths measured by the two nephelometers are highly consistent (Fig. S2). The slopes of the linear fittings are close to 1, and the squared Pearson's correlation coefficient (R^2) is also close to 1, indicating that the two nephelometers are consistent with each other.



10 **Figure S2: Checking the consistency of the two nephelometers: (a) scattering coefficient at 635 nm, (b) scattering coefficient at 525 nm, (c) scattering coefficient at 450 nm, (d) backscattering coefficient at 635 nm, (e) backscattering coefficient at 525 nm, and (f) backscattering coefficient at 450 nm measured by the two nephelometers. The linear regression function, the squared Pearson's correlation coefficient (R^2), and root-mean-square error (RMSE) are given in the upper-left corner of each panel.**



15 **Figure S3: The relationship between the uncorrected $f(RH=85\%,525nm)$ and corrected $f(RH=85\%,525nm)$. The solid red line represents the linear least square regression. The blue line is the line of 1:1. The linear regression function and the Pearson's correlation coefficient (R) are given in the bottom-right corner of the panel.**

Figure S4 shows the result of the calibration of the high-resolution humidified nephelometer system with ammonium sulphate. It shows a measured humidogram of $f(\text{RH}, 525\text{nm})$ for ammonium sulphate, where x-axis represents the RH in the optical chamber of humidified nephelometer. When RH is lower than 79.41%, the values of $f(\text{RH}, 525\text{nm})$ are consistently remained about 1. The literature value for the deliquescence relative humidity (DRH) of ammonium sulphate is 80% at 298K (Cheung et al., 2015). The measured phase transition occurs at $\text{RH}=80.37\%$. It indicates that the RH inside the nephelometer chamber is correct and that the system is functioning properly.

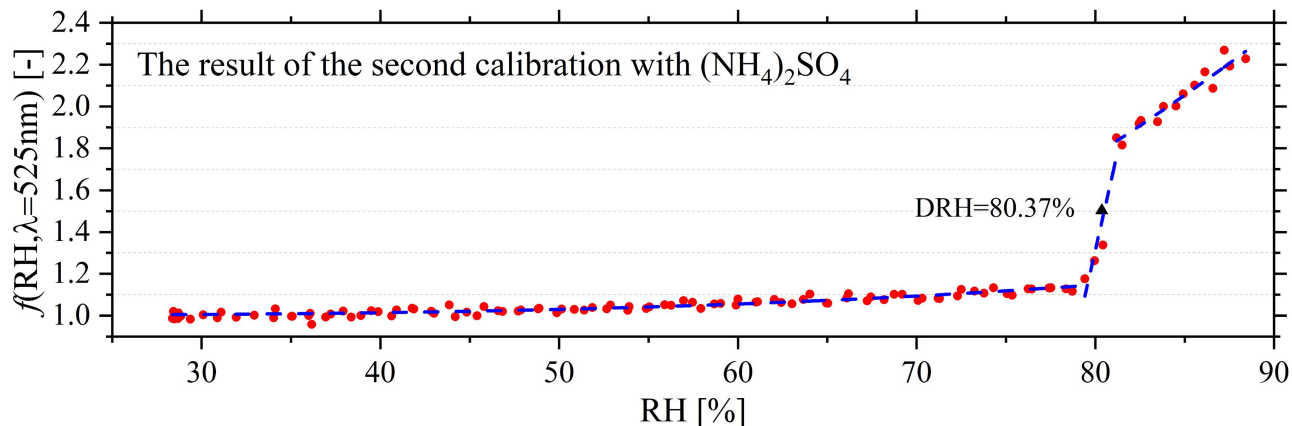


Figure S4: Deliquescence results of the pure ammonium sulfate aerosol generated in the laboratory. The $f(\text{RH})$ vs. RH of ammonium sulfate particles at $\lambda=525\text{nm}$. The phase transition at deliquescence occurred at about $\text{RH}=80.37\%$.

25

Table S1: Statistical values of $f(\text{RH} = 85\%)$ at 450, 525, and 635 nm (STD: standard deviation; prctl: percentile; N: sample size).

| λ | mean | STD | 90th prctl | 75th prctl | median | 25th prctl | 10th prctl | N |
|-----------|------|------|------------|------------|--------|------------|------------|-----|
| 450 nm | 1.57 | 0.10 | 1.66 | 1.64 | 1.59 | 1.52 | 1.41 | 294 |
| 525 nm | 1.64 | 0.13 | 1.75 | 1.72 | 1.67 | 1.59 | 1.44 | 294 |
| 635 nm | 1.70 | 0.15 | 1.84 | 1.79 | 1.74 | 1.65 | 1.46 | 294 |

With increasing wavelength, both the mean value and the standard deviation of $f(\text{RH} = 85\%)$ increase slightly. The hygroscopic enhancement factor is wavelength dependent, a property useful for estimating aerosol radiative forcing. Figure S5 shows the histogram for $f(\text{RH} = 85\%, 525 \text{ nm})$ overlaid with the Gaussian-fit curve (in green). Also shown are two other Gaussian-fit curves, i.e., for $f(\text{RH} = 85\%, 450 \text{ nm})$ and $f(\text{RH} = 85\%, 635 \text{ nm})$.

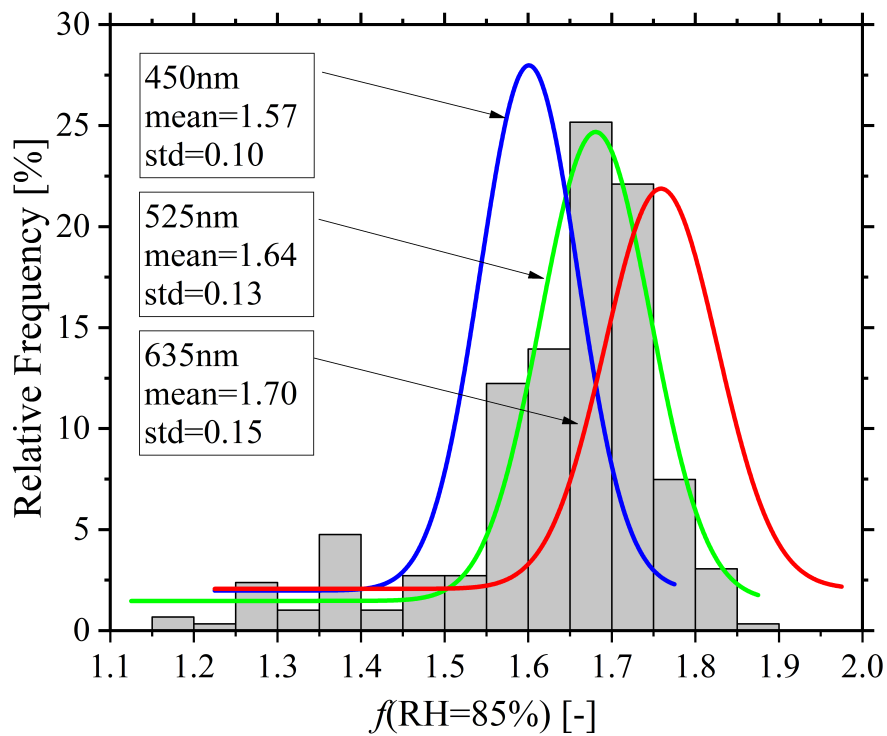
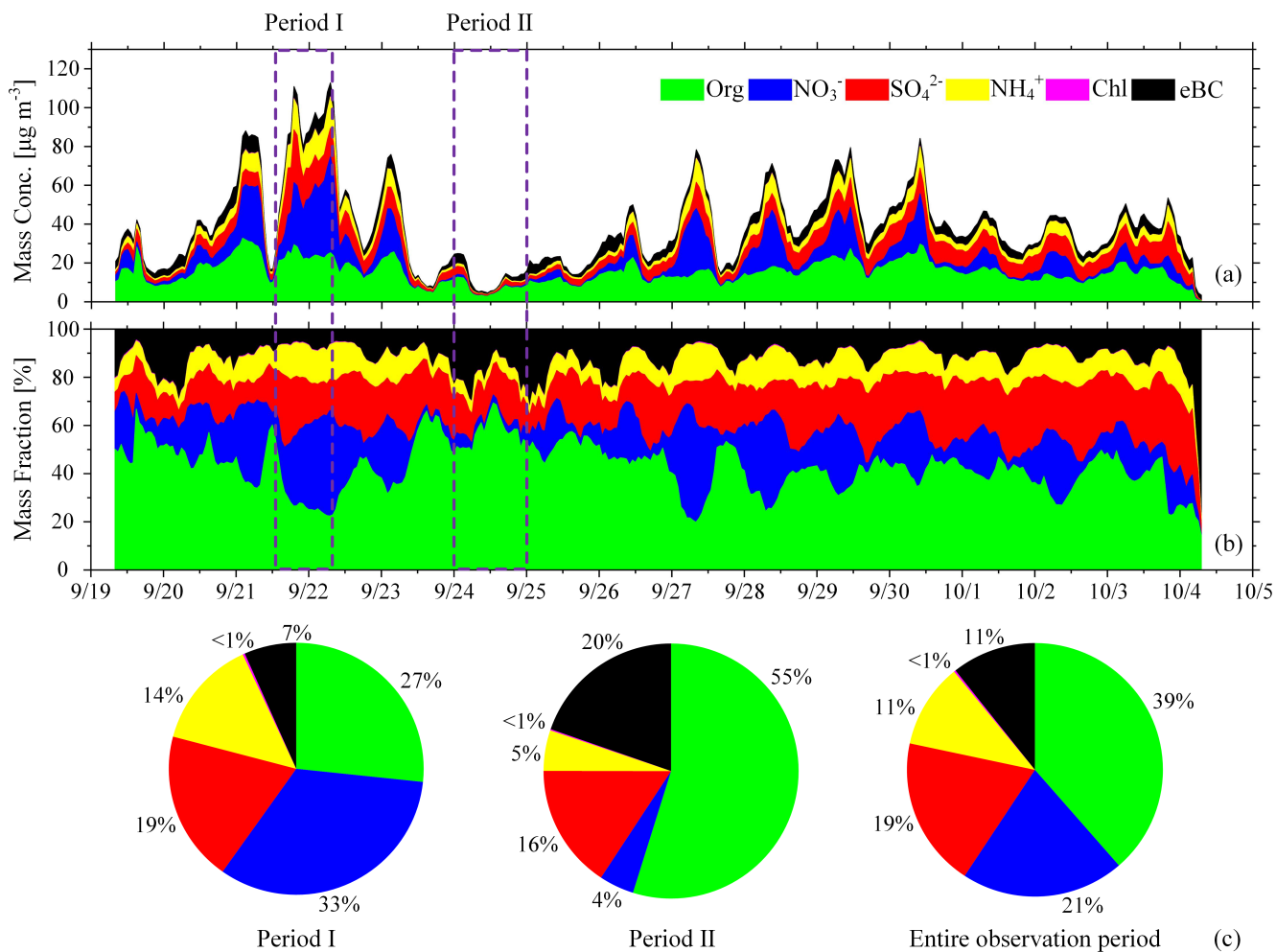


Figure S5: Frequency distribution histogram of $f(\text{RH} = 85\%, 525 \text{ nm})$ overlaid with Gaussian-fit curves based on statistical analyses of $f(\text{RH} = 85\%, 450 \text{ nm})$, $f(\text{RH} = 85\%, 525 \text{ nm})$, and $f(\text{RH} = 85\%, 635 \text{ nm})$, represented by blue, green, and red curves, respectively.



35

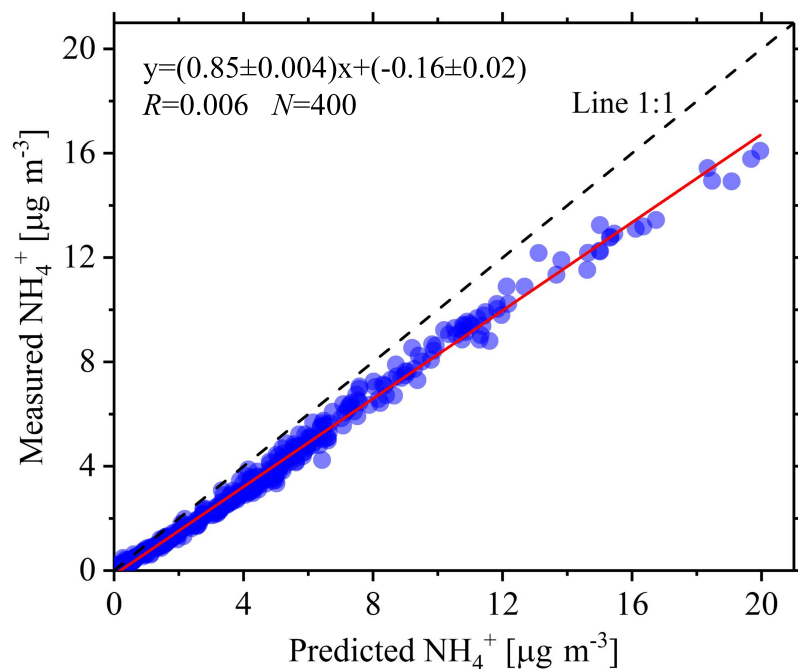
Figure S6: Time series of (a) mass concentrations (unit: $\mu\text{g m}^{-3}$) and (b) mass fractions of NR-PM_{2.5} species (unit: %), i.e., organics, nitrate, sulfate, ammonium, chloride and the equivalent black carbon (eBC). The timescale is Beijing time (UTC + 8 h). The date in this figure is in the month/day format. The pie charts in (c) show the average chemical composition of NR-PM_{2.5} for Period I (the pie chart on the left), Period II (the pie chart in the middle), and the entire observation period (the pie chart on the right).

40 Aerosol acidity is one of the most important factors affecting the hygroscopicity of aerosols. The pH of ambient aerosols is estimated by comparing the mass concentrations of NH_4^+ _{measured} and NH_4^+ _{predicted}, which is the amount of ammonium needed to thoroughly neutralize chloride, nitrate, and sulfate ions (Sun et al., 2012):

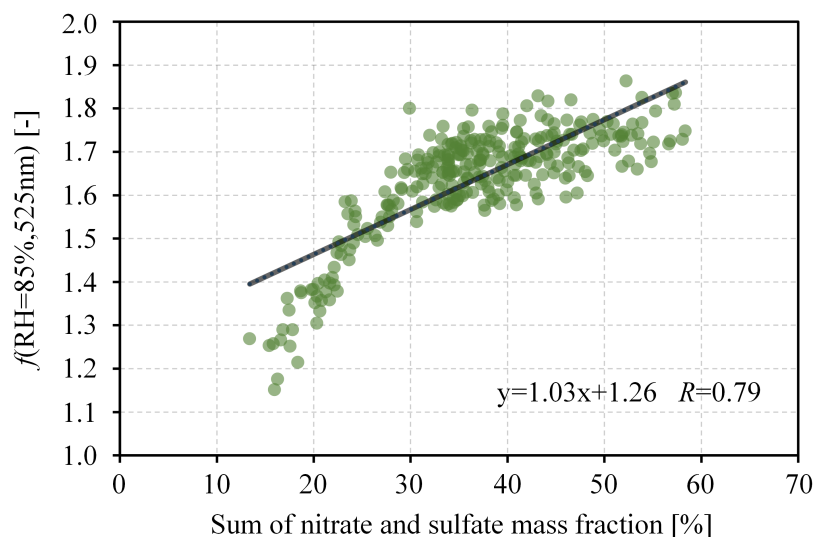
$$\text{NH}_4^+_{\text{predicted}} = 18 \times \left(2 \times \frac{\text{SO}_4^{2-}}{96} + \frac{\text{NO}_3^-}{62} + \frac{\text{Cl}^-}{35.5} \right). \quad (1)$$

45 Figure S7 shows NH_4^+ _{measured} as a function of NH_4^+ _{predicted}. The regression slope is 0.85 ± 0.004 , which is slightly less than 1. This implies that the ambient NH_3 was not sufficient to neutralize HCl, HNO_3 , and H_2SO_4 . PM_{2.5} aerosols at the

observatory in suburban Beijing were thus faintly acidic during the observation period, benefitting the hygroscopic enhancement of ambient aerosols.



50 **Figure S7:** Measured ammonium concentration as a function of predicted ammonium calculated using Eq. (1). The linear regression function, Pearson's correlation coefficient (R), and sample size (N) are given in the panel. The dashed line is the 1:1 line, and the red line is the best-fit line from linear regression through the data points.



55 **Figure S8:** Hygroscopic enhancement factor $f(\text{RH} = 85\%, 525\text{nm})$ as a function of the sum of nitrate and sulfate mass fractions. The linear regression function and the Pearson's correlation coefficient (R) are given in the bottom-right corner of the panel. The black line is the best-fit line from linear regression through the data points.

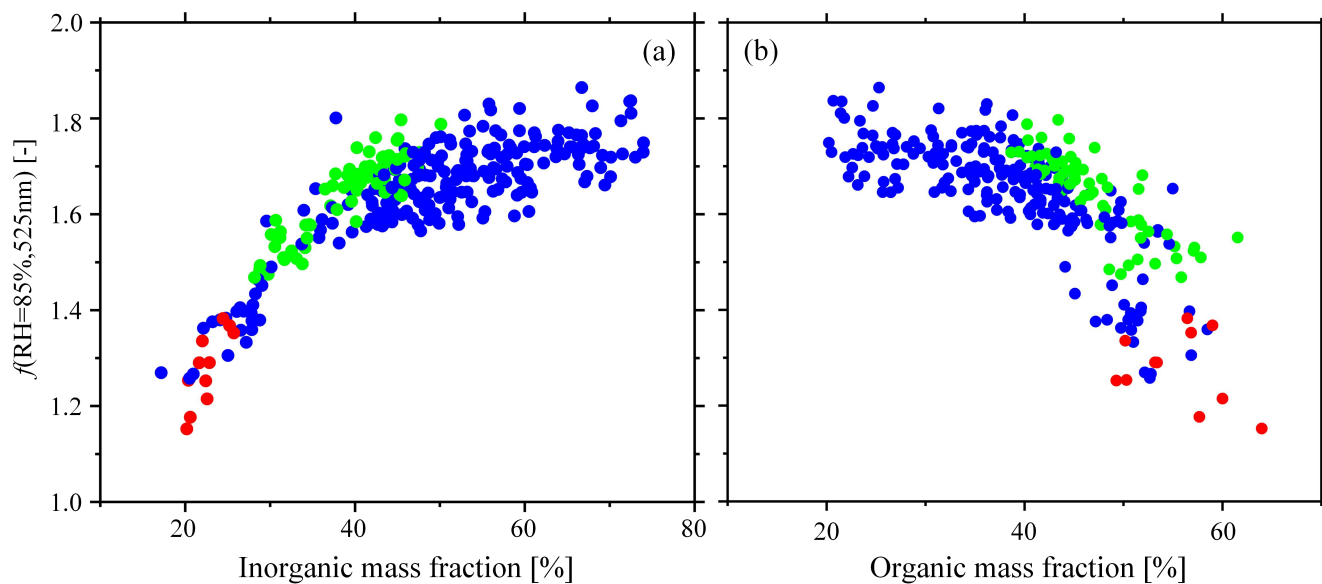
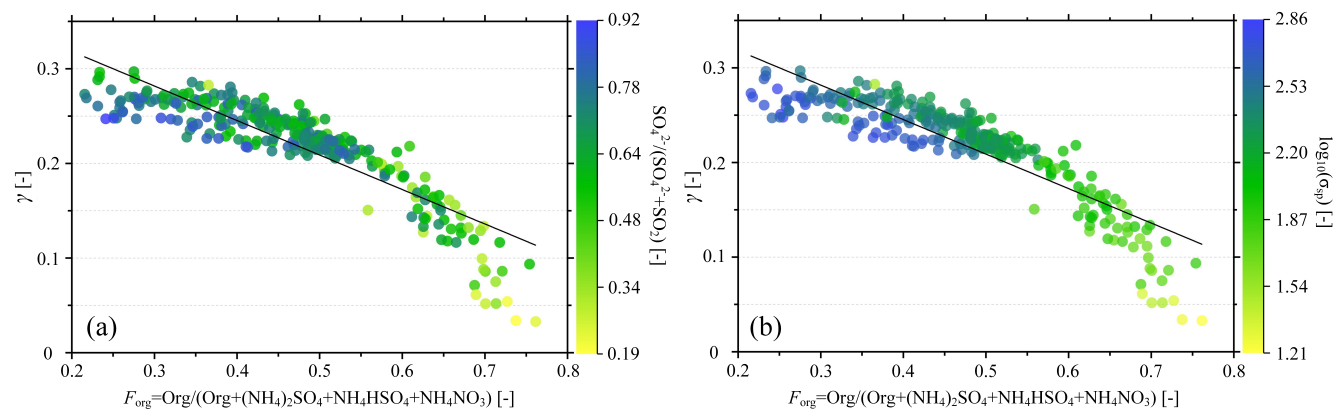
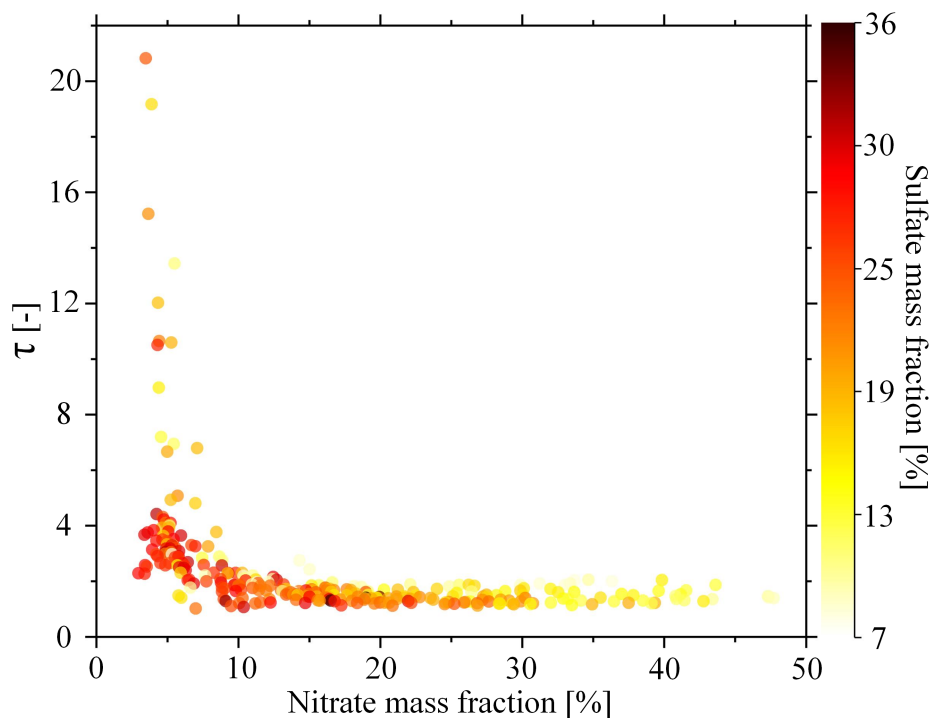


Figure S9: Hygroscopic enhancement factor $f(\text{RH} = 85\%, 525\text{nm})$ as a function of (a) inorganic matter mass fraction and (b) organic matter mass fraction. The green dots represent deliquescence, the blue dots represent non-deliquescence and the red dots represent those data points with high systematic errors.



60

Figure S10: γ as a function of F_{org} ($\text{Org}/(\text{Org} + (\text{NH}_4)_2\text{SO}_4 + \text{NH}_4\text{HSO}_4 + \text{NH}_4\text{NO}_3)$), colored by (a) the $\text{SO}_4^{2-}/(\text{SO}_4^{2-} + \text{SO}_2)$ molar ratio and (b) $\log_{10}(\sigma_{\text{sp}})$.



65 **Figure S11: Scatter plot of the steepness index (τ) as a function of the nitrate mass fraction (unit: %), colored by the sulfate mass fraction (unit: %).**

References

- Cheung, H. H. Y., Yeung, M. C., Li, Y. J., Lee, B. P., and Chan, C. K.: Relative humidity-dependent TDMA measurements of ambient aerosols at the HKUST supersite in Hong Kong, China, *Aerosol Sci. Tech.*, 49, 643–654, <https://doi.org/10.1080/02786826.2015.1058482>, 2015.
- 70 Sun, Y., Wang, Z., Dong, H., Yang, T., Li, J., Pan, X., Chen, P., and Jayne, J. T.: Characterization of summer organic and inorganic aerosols in Beijing, China with an aerosol chemical speciation monitor, *Atmos. Environ.*, 51, 250–259, <https://doi.org/10.1016/j.atmosenv.2012.01.013>, 2012.